The Effect of Flow Velocity on the Effectiveness of Porous Tubes as Underwater Current Deflectors in Bridge Pier Scour Control

Nenny
Department of Civil Engineering, Universitas Muhammadiyah Makassar, Indonesia
nenny@unismuh.ac.id (corresponding author)

Hamzah Al Imran
Department of Civil Engineering, Universitas Muhammadiyah Makassar, Indonesia
hamzah@unismuh.ac.id

Andi Makbul Syamsuri
Department of Water Resources Engineering, Universitas Muhammadiyah Makassar, Indonesia
amakbulsyamsuri@unismuh.ac.id

Abd Rakhim Nanda
Department of Water Resources Engineering, Universitas Muhammadiyah Makassar, Indonesia
abd.rakhimnanda@unismuh.ac.id

Muhammad Faisal
Department of Informatics, Universitas Muhammadiyah Makassar, Makassar, Indonesia
muhfaisal@unismuh.ac.id

Muhammad Syafaat S. Kuba
Department of Water Resources Engineering, Universitas Muhammadiyah Makassar, Indonesia
syafaat_skuba@unismuh.ac.id

Received: 7 March 2026 | Revised: 2 April 2026 | Accepted: 21 April 2026

 DOI: https://doi.org/10.48084/etasr.18590

ABSTRACT

Local scour at bridge piers is a major cause of foundation exposure and failure during high-energy flows. Because flow velocity governs downflow and horseshoe-vortex strength at the pier base, scour countermeasures should be assessed across hydraulic intensities. This study evaluates how increasing velocity affects porous-tube Underwater Current Deflectors (UCDs) in reducing near-pier flow and scour depth after 90 min of testing, comparing triangular and reinforced triangular layouts. Flume tests were performed in an 8.50 m × 0.51 m rectangular channel with a mid-channel cylindrical pier. Two discharges (Q1 = 0.00352 m^3/s and Q2 = 0.00395 m^3/s) were run for an unprotected pier and for protection using porous-tube triangular and reinforced triangular UCDs. The longitudinal velocities were measured at stations P1–P15 and scour along the pier centerline at P1–P12 after each run. Compared with the unprotected case, the UCDs reduced the centerline-averaged longitudinal velocity measured along stations P1-P15 by 27–35% at Q1 and 36–39% at Q2. Maximum scour decreased from 6.1 cm (Q1) and 9.0 cm (Q2) to 3.3–3.5 cm (Q1) and 3.5–3.9 cm (Q2), i.e., 43–46% and 57–61% reductions, respectively, with the reinforced design consistently yielding the lowest scour. The results indicate that porous-tube UCDs mitigate scour without full bed armoring, and reinforcement sustains effectiveness at higher velocities.

Keywords-porous tube; underwater current deflector; bridge pier scour; flow velocity; flume experiment

I. INTRODUCTION

Local scour at bridge piers is one of the primary causes of bridge foundation instability and structural failure in riverine environments [1]. Bridge foundations are routinely exposed to complex three-dimensional flow structures that intensify bed shear stress and promote localized sediment removal at structural interfaces. When a bridge pier interrupts the approach flow, a characteristic downflow develops along the upstream face of the pier and interacts with boundary layer separation to generate a horseshoe vortex system around the pier base [2]. The vortex-induced pressure gradients and associated bed-material entrainment create a scour hole that can expand in depth and planform until an equilibrium between erosive capacity and sediment supply is reached. Because even modest scour depths can reduce foundation embedment and compromise structural safety, bridge-pier scour remains a central concern in hydraulic engineering and infrastructure resilience [3]. Since pier scour is frequently implicated in bridge damage and collapse, reliable detection and monitoring methods are emphasized in practice.

Experimental work under pressurized flow conditions indicates that scour behavior can change during floods when the flow interacts with the bridge deck [4]. The difficulty of scour management lies in its strong dependence on hydraulic intensity and the interaction between the flow regime and bed mobility. Previous research has highlighted that the available predictive equations for clear-water and live-bed scour can show wide variability, reflecting sensitivity to flow velocity, sediment characteristics, and structural geometry. Complementing this, experimental investigations into pier-shape effects have demonstrated that geometry modifies the local flow field and spatial distribution of scour depth. Under live-bed conditions, sediment supply alters scour evolution. Authors in [5] showed that sediment feeding can influence scour development around circular bridge piers, implying that scouring and partial infilling may co-occur, depending on upstream bedload availability. In addition to reviews about predictive equations, decision frameworks have been proposed to rank and select local scour formulas using field data, statistics, and sensitivity analyses [6]. Data-driven models, such as the Adaptive Network-based Fuzzy Inference System (ANFIS) and gene expression programming, have also shown strong predictive capability for both clear-water and live-bed conditions when trained on dimensionless hydraulic and sediment parameters [7]. On the process-modeling side, Computational Fluid Dynamics (CFD) based approaches are increasingly used to resolve near-pier shear stresses and reproduce scour around complex supports [8]. Moreover, the performance of 1D/2D hydraulic tools for predicting pier scour across pier shapes and conditions has been evaluated.

Real-world bridge environments introduce additional complexities related to debris accumulation and proximity to channel boundaries [9]. Debris blockage can increase the effective obstruction at a pier and intensify turbulence, thereby exacerbating local scour processes. Likewise, debris accumulation near riverbanks can modify scour evolution by altering flow separation and local contraction effects. These interacting mechanisms highlight the importance of developing countermeasures capable of maintaining effectiveness under disturbed hydraulic conditions and variable sediment transport regimes. Experimental investigations have shown that structural devices, such as collars installed around cylindrical bridge piers, can significantly reduce scour depth by disrupting horseshoe vortices and modifying near-bed flow patterns [10]. However, real river environments remain highly dynamic, and additional factors, such as instream wood accumulation, debris interactions, and channel morphology, can further influence scour development. Instream wood accumulation at bridges is a key driver of flood hazards [11], while refined methods have been proposed to quantify debris-induced scour using debris factors that account for debris dimensions and elevation. Numerical investigations have further indicated that debris interaction and multi-bridge configurations can amplify contraction scour and modify local scour patterns [12]. Complex flow fields, such as sharp channel bends and multiple-pier arrangements, can intensify three-dimensional flow structures and shift scour locations, underscoring the importance of considering site-specific hydraulic conditions beyond simplified straight-channel assumptions.

Bridge piers are highly vulnerable to local scour, particularly in morphodynamically active river environments such as those commonly found in Indonesia. Previous laboratory and field-oriented studies have investigated scour processes around bridge piers and evaluated structural interventions designed to modify near-pier flow patterns [13]. Alongside physical experimentation, numerical modeling tools, such as HEC-RAS and iRIC/Nays2DH simulations, have been employed to analyze flow–structure interactions and assess the effectiveness of scour mitigation devices [14]. At the reach scale, integrated hydrologic–hydraulic analyses indicate that scour risk often intensifies during extreme discharge events, especially in ungauged basins characterized by high hydrological uncertainty.

Consequently, various mitigation approaches, including bed armoring, flow-altering structures, and upstream protection elements, have been proposed. For instance, upstream protective piles can weaken the vortex structures responsible for scour development around cylindrical bridge piers. Empirical and experimental methods are crucial for predicting scour depth and evaluating the effectiveness of these countermeasures, whereas research has highlighted sustainable armoring solutions, such as gabion mattresses, which can significantly reduce pier scour.

Among flow-altering interventions, permeable and semi-permeable devices are attractive because they redirect near-bed flow while allowing partial flow-through, thereby reducing the risk of excessive contraction and unintended upstream afflux [15]. Local studies on shape-based modifications, such as curtains or wings, have shown that altering the near-pier geometry can substantially change scour patterns. Such results are consistent with the broader understanding that velocity and local flow orientation strongly control the initiation and evolution of scour holes. These insights motivate the development of practical devices that can be installed around existing piers to modify flow trajectories and weaken scour-driving vortical structures without requiring full-bed armoring.

Evidence from porous and permeable structures indicates that porosity can reduce the intensity and variability of wall shear stress and yield more stable scour evolution compared with solid obstacles [16]. Similarly, permeable flow-training devices, such as angled spur dikes, show substantial attenuation of temporal scour development under both steady and unsteady flows, with benefits often increasing with permeability [17]. Detailed measurements of the turbulent flow field around non-circular piers and sorting processes in graded beds further indicate that geometry, turbulence statistics, and grain size distribution jointly control scour-hole shape and evolution.

Despite these advances, two persistent gaps limit the practical deployment of many flow-altering countermeasures. First, devices are often evaluated under a single hydraulic condition, leaving uncertainty about how performance scales with flow velocity, which is a key driver of vortex strength and sediment entrainment capacity. Second, countermeasures must mitigate scour without producing excessive blockage or deposition patterns that may transfer risk downstream.

Porous-tube Underwater Current Deflectors (UCDs) represent a promising class of devices because their porosity can dissipate momentum and redirect near-bed flow while avoiding complete obstruction. However, the velocity dependence of porous-tube UCD effectiveness and the extent to which structural reinforcement improves reliability under stronger flows remain insufficiently quantified. These gaps motivate the development of velocity-dependent laboratory datasets that can be used to calibrate advanced numerical simulations and support the translation of scour bathymetry into structural assessments.

The objective of this study is to analyze the hydrodynamic characteristics and scour patterns around a cylindrical bridge pier in the presence of porous-tube UCD under two discharges representing different flow velocities. Two configurations were evaluated: a triangular porous-tube UCD and a reinforced triangular porous-tube UCD. The study addresses three questions: (i) How do porous-tube UCDs modify the longitudinal velocity distribution along the pier centerline? (ii) How do these velocity changes translate into reductions in the maximum and spatially distributed scour depth? (iii) Does reinforcement provide measurable performance benefits as flow velocity increases? The outcomes are intended to support evidence-based selection and refinement of practical scour countermeasures for riverine bridges in high-current environments.

II. MATERIALS AND METHODS

This study employed controlled laboratory flume experiments to evaluate the hydraulic and morphodynamical effectiveness of porous-tube UCDs in mitigating local scour at a cylindrical bridge pier. Experiments were conducted to isolate the effect of flow velocity (via two discharges) on deflector performance and to compare a triangular porous-tube UCD with a reinforced triangular configuration. The workflow consisted of establishing a steady approach flow, measuring longitudinal velocity distributions along predefined stations, draining the flume, and surveying post-test bed topography to quantify local scour and deposition.

The experimental workflow of this study is illustrated in Figure 1.

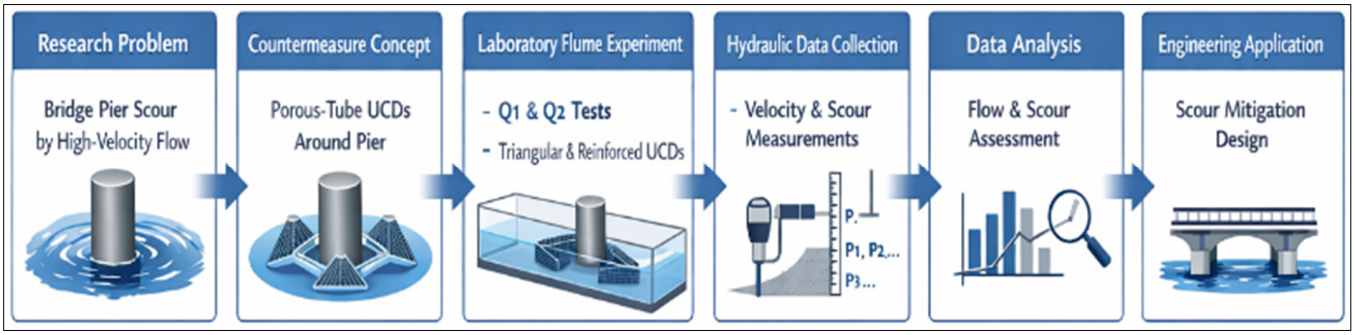

Fig. 1. Research framework illustrating the experimental workflow of this study.

A. *Experimental Setup and Hydraulic Similarity*

Experiments were conducted in a straight rectangular open-channel flume under steady subcritical flow conditions. The flume length and width were 8.50 m and 0.51 m, respectively. A rigid cylindrical pier model was installed at the channel centerline to represent a common pier type. The test section was filled with uniform sand bed material and leveled prior to each run to provide repeatable initial conditions. According to the results of the material testing, the sand used in this study was classified as silty sand with a median grain size (dm) of 1.20 mm, a mud content of 3.71%, a specific gravity of 2.68, and a fineness modulus of 2.321. Geometric and dynamic similarities were achieved through standard free-surface scaling, preserving the dominant balance between the inertial and gravitational forces in the modeled flow-structure interaction. The flow conditions during the experiment were initially characterized based on the Froude number (Fr). At the bridge pier, the flow regime was identified as supercritical with an average Fr value of 1.229. However, following the installation of the UCD model, the flow regime transitioned to subcritical, as indicated by an average Fr value of 0.569.

Although the Froude similarity is the standard for free-surface modeling, scale effects and time-to-equilibrium considerations should be considered when extrapolating laboratory scouring results to field applications, as depicted in Figure 2.

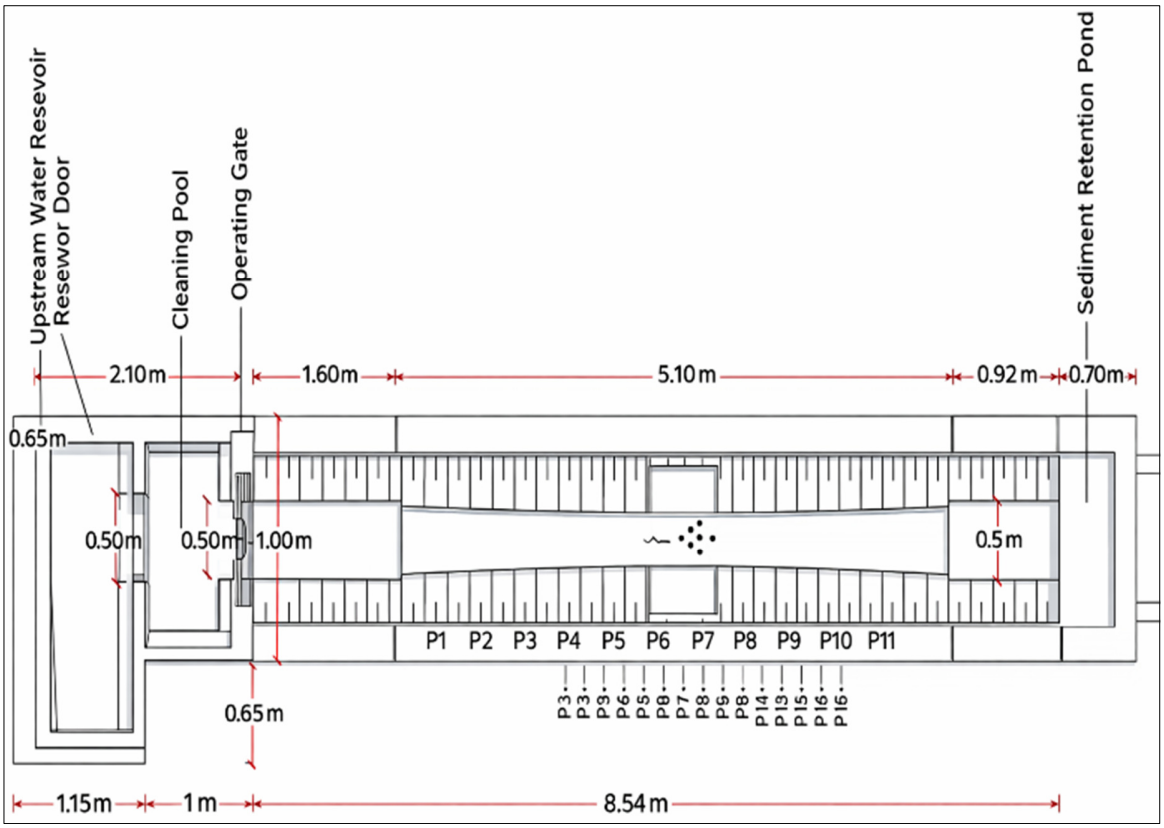

Fig. 2. Open-channel flume model and test-section arrangement.

B. Instrumentation and Measurement Techniques

The flow velocity was measured using a calibrated electromagnetic current meter (Valeport Model 801, accuracy ±0.5% of reading) at multiple longitudinal stations (P1–P15). Measurements were taken at 60% of the water depth from the bed, corresponding to the depth-averaged velocity location for turbulent open-channel flow. Each measurement was recorded over a 30-s sampling period to obtain a stable mean value.

Water depth was monitored using point gauges to maintain target flow conditions and support discharge verification. After each run, the flume was drained carefully, and the bed elevations were surveyed using depth probes/bed profilers to obtain scour depth distributions (P1–P12) around the pier. Instruments were checked for zero offsets prior to each experiment, and repeated readings were taken when necessary to reduce observational uncertainty. The adopted measurement strategy is consistent with commonly reported laboratory and field practices for scour observation and documentation.

C. Porous Tube UCD Configuration

The porous tube UCD was fabricated from acrylic to provide hydraulic resistance while remaining lightweight and straightforward to install. The porous structure allows partial flow through, intended to dissipate momentum and redistribute near-bed shear stresses rather than fully blocking the approach flow. Two geometries were evaluated: (i) a triangular porous-tube UCD and (ii) a reinforced triangular porous-tube UCD (Figures 3-6).

The reinforced triangular UCD was fabricated by adding three longitudinal acrylic stiffeners (5 mm width × 10 mm height) at the internal vertices of the triangular frame, as displayed in Figures 5 and 6. These stiffeners increased the structural rigidity without altering the external dimensions or the effective porosity (35%). The reinforcement was designed to prevent deformation of the porous tubes under higher flow velocities (Q2) and to maintain consistent flow-redirection characteristics throughout each experimental run.

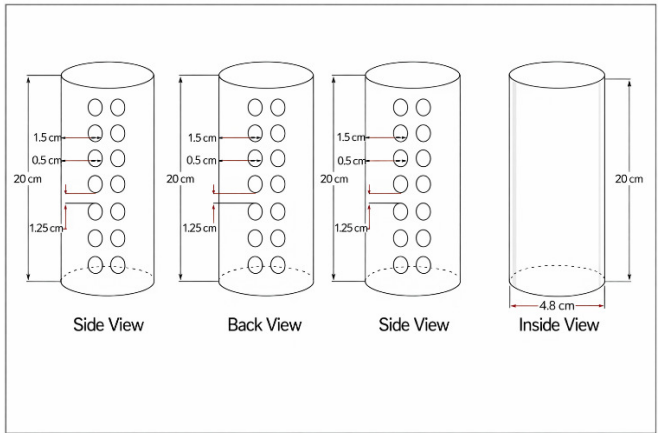

Fig. 3. Porous-tube UCD concept.

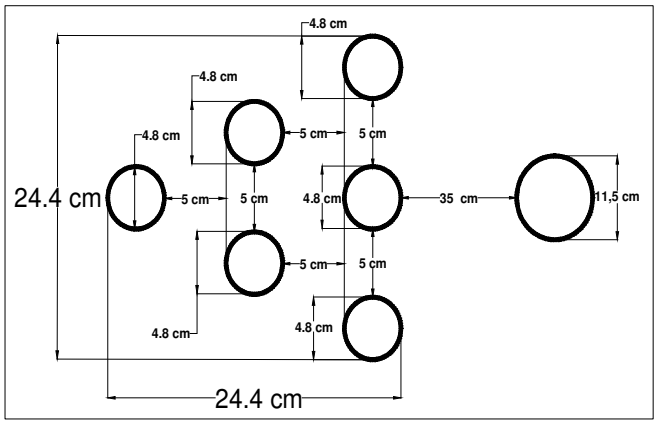

Fig. 4. Porous-tube UCD configurations.

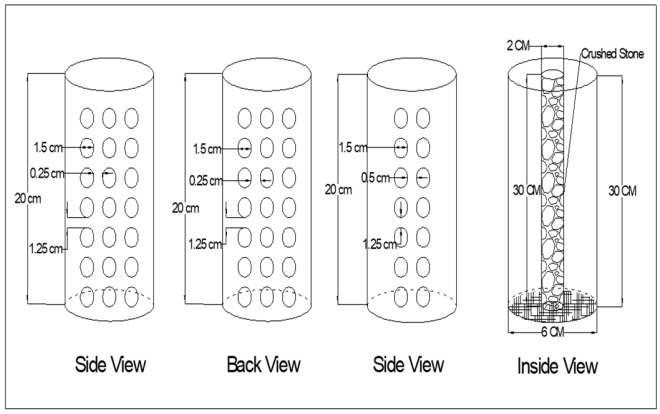

Fig. 5. Reinforced triangular porous-tube UCD configuration.

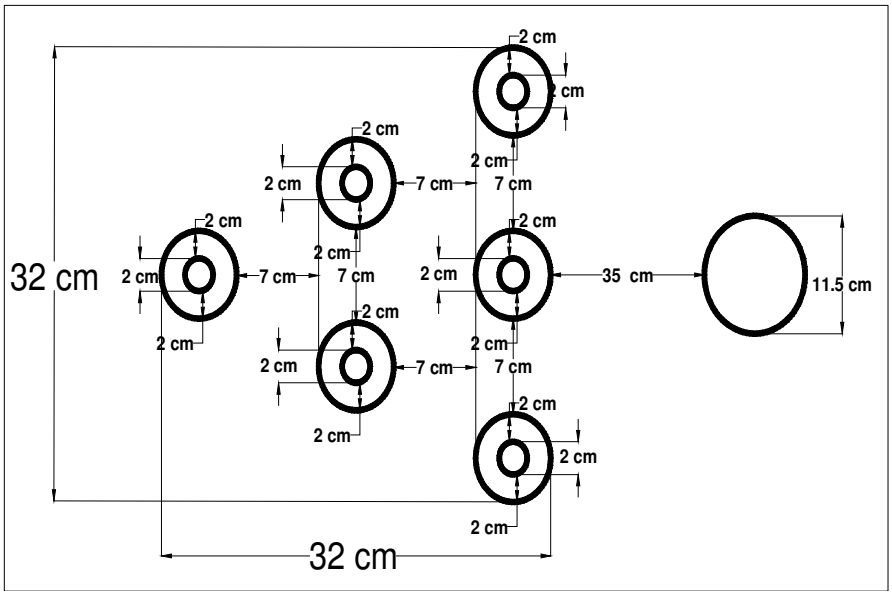

Fig. 6. Reinforced triangular UCD installed around the pier in the flume.

TABLE I. HYDRAULIC CONDITIONS AND FLUME DIMENSIONS USED IN THE EXPERIMENTS

Description	Value
Discharge (Q1) (m^3/s)	0.00352
Discharge (Q2) (m^3/s)	0.00395
Time	30 min
Time	60 min
Time	90 min
Channel length model	8.50 m
Channel width model	0.51 m

Each test was conducted under two scenarios: (a) baseline conditions with an unprotected pier and (b) protected conditions with a porous-tube UCD installed. Two discharges were imposed: Q1 = 0.00352 m^3/s and Q2 = 0.00395 m^3/s (Table I) to represent increasing hydraulic intensity. For each discharge and configuration, the flow was allowed to stabilize before the velocity measurements were collected. Runs were maintained for observation intervals of 30, 60, and 90 min. Preliminary tests indicated that under clear-water scour conditions, the scour depth reached approximately 90% of the equilibrium value within 90 min. Therefore, the 90-min duration was considered sufficient for comparative assessment of countermeasure effectiveness. Dye tracing was used qualitatively to observe changes in near-pier trajectories and separation zones induced by the deflectors.

D. Data Processing and Performance Metric

The performance was evaluated by comparing (i) the longitudinal velocity distributions with and without UCD (Tables II–III and Figures 7–8) and (ii) the corresponding scour depth profiles (Tables IV–V and Figures 9–16). In addition to point measurements, summary indicators were computed for each discharge and configuration, including spatially averaged velocity reduction along the observation line and reduction in maximum scour depth relative to the unprotected pier. These metrics provided a transparent, velocity-dependent assessment of countermeasures. Each experimental condition was repeated three times to ensure repeatability and to account for potential variability in bed preparation and flow conditions. The reported

velocity and scour values represent the arithmetic mean of the three runs. The standard deviations were calculated for each measurement point to assess the repeatability of the experiments. The average coefficient of variation was less than 5%, indicating acceptable consistency.

E. Scour-Depth Measurement and Bed-Topography Survey

After velocity and stage measurements were completed for a given run, the flow was stopped, and the channel was slowly drained to preserve bed morphology. The local scour depth (ds) was measured by referencing post-run bed elevations to the initial level bed along the pier centerline and adjacent points. The results are presented in Figure 7.

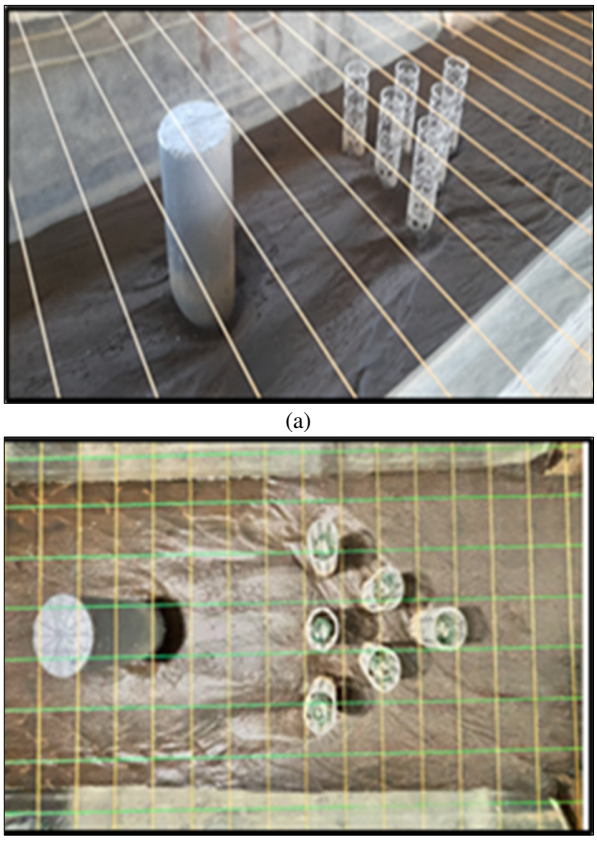

(a)

(b)

Fig. 7. Representative local scour patterns around the pier with and without porous tube UCD protection: (a) baseline pier and (b) pier with UCD.

The resulting longitudinal scour/deposition profiles were used to identify the maximum scour depth, scour hole extent, and deposition zones downstream of the pier and deflector.

III. RESULTS AND DISCUSSION

A. Velocity Distribution and Flow Modification by Porous-Tube UCD

Two discharges were imposed to represent the increasing hydraulic intensity. As expected, the higher discharge Q2 produced higher approach velocities than Q1 along the observation line for the unprotected pier. The measured longitudinal velocities (P1–P15) provide a consistent basis for evaluating how each porous-tube UCD configuration redistributes momentum and for linking these hydrodynamic changes to scour outcomes, as illustrated in Tables II and III, and Figures 8 and 9.

For Q1 (0.00352 m^3/s), the baseline velocities near the pier ranged from 0.533 to 0.667 m/s. The installation of the triangular and reinforced triangular UCD reduced the velocities along much of the mid to downstream observation line. When averaged over the measurement stations, the reinforced UCD achieved a 34.8% reduction in longitudinal velocity relative to the unprotected pier, compared with 27.0% for the unreinforced triangular UCD.

TABLE II. LONGITUDINAL FLOW VELOCITY (V) ALONG THE OBSERVATION LINE FOR DISCHARGE Q1

Measuring distance	Bridge pillar	Reinforced triangular UCD	Triangular UCD
	Flow velocity (v) (m/s)		
P1	0.633	0.567	0.633
P2	0.567	0.567	0.567
P3	0.600	0.567	0.567
P4	0.600	0.567	0.533
P5	0.667	0.567	0.533
P6	0.633	0.533	0.533
P7	0.633	0.400	0.467
P8	0.633	0.367	0.467
P9	0.633	0.267	0.433
P10	0.600	0.250	0.400
P11	0.533	0.233	0.333
P12	0.567	0.267	0.300
P13	0.600	0.267	0.300
P14	0.633	0.267	0.300
P15	0.600	0.267	0.300

TABLE III. LONGITUDINAL FLOW VELOCITY (V) ALONG THE OBSERVATION LINE FOR DISCHARGE Q2

Measuring distance	Bridge pillar	Reinforced triangular UCD	Triangular UCD
	Flow velocity (v) (m/s)		
P1	0.667	0.633	0.667
P2	0.600	0.633	0.567
P3	0.633	0.600	0.567
P4	0.633	0.567	0.533
P5	0.700	0.567	0.533
P6	0.733	0.567	0.533
P7	0.667	0.367	0.433
P8	0.700	0.400	0.400
P9	0.667	0.300	0.367
P10	0.650	0.350	0.350
P11	0.700	0.267	0.300
P12	0.733	0.233	0.333
P13	0.700	0.267	0.333
P14	0.733	0.233	0.300
P15	0.733	0.233	0.333

The velocity reductions were not spatially uniform. The upstream stations remained relatively high, indicating that the deflectors primarily modified the near-pier and downstream regions rather than suppressing the entire approach flow. This pattern is relevant for scour control because local scour is

governed by near-bed velocity gradients and vortex intensity around the pier base, rather than by bulk flow alone. Figure 7 indicates that both porous-tube UCDs decrease downstream velocities, consistent with momentum dissipation through the porous elements and partial redirection of streamlines around the pier. The reinforced configuration provided the most pronounced attenuation at downstream stations, suggesting improved stability of the deflector geometry under flow and more consistent energy dissipation across the protected region. The Q1 results showed that porous tube UCDs can substantially weaken the longitudinal velocity field in regions that most strongly influence near-bed shear and vortex formation at the pier base.

This reduction in velocity after deflector placement highlights the device's efficiency in controlling flow dynamics. It also suggests that the reinforced model has a stronger ability to reduce flow speed, which is critical for improving sediment transport control and minimizing erosion around structures such as bridge piers.

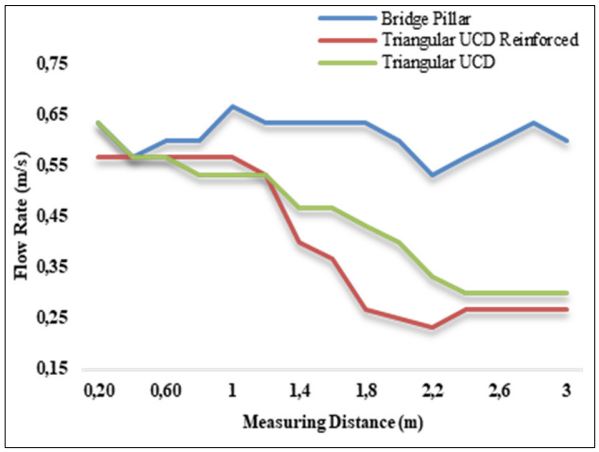

Fig. 8. Comparison of flow velocity for discharge Q1.

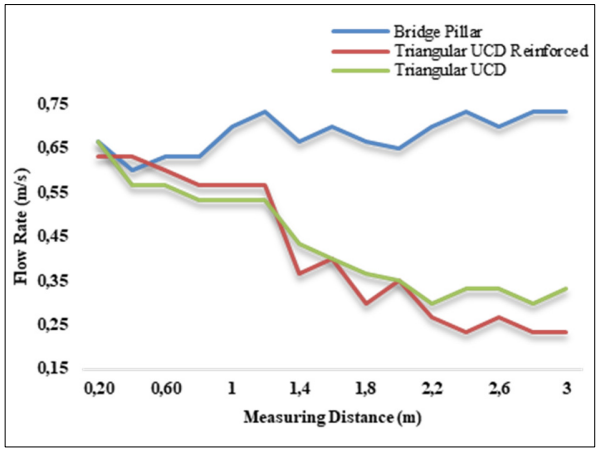

Fig. 9. Comparison of flow velocity for discharge Q2.

For Q2 (0.00395 m^3/s), the baseline velocities increased to 0.600–0.733 m/s, confirming a higher-energy flow field. Both UCDs continued to reduce downstream velocities. On a spatially averaged basis, longitudinal velocity decreased by 39.3% for the reinforced UCD and 36.1% for the triangular UCD relative to the unprotected pier, indicating that reinforcement retained a performance advantage as discharge increased. This reduction in flow velocity after the installation of the deflector demonstrates the effectiveness of this behavior, which is consistent with the established scour mechanism in which near-bed acceleration, downflow, and the horseshoe vortex system control sediment entrainment at the pier base. The observed scour reduction with porous-tube UCD installations can be attributed to three interacting mechanisms:

1. Momentum dissipation: The porous structure reduces the near-bed longitudinal velocity by 27–39% (Tables II and III), directly weakening the approach flow energy available for sediment entrainment.
2. Vortex modification: Flow redirection around the porous array disrupts the formation of the horseshoe vortex at the pier base, as qualitatively confirmed by dye-tracing observations during the experiments.
3. Shear stress redistribution: Partial flow transmission through the porous tubes prevents the formation of strong contraction jets downstream of the pier, promoting more uniform bed shear stress distribution and reducing localized scour. Current deflectors are excellent in reducing flow speed, which is critical for controlling sediment movement and minimizing the erosive impact on structures such as bridge piers. The comparison of velocity values before and after the deflector placement highlights the positive influence of these models in altering flow dynamics.

The persistence of attenuation at Q2 suggests that porous-tube installations can remain effective under increased hydraulic loading, although the absolute approach velocity still controls the potential erosive capacity at the bed. Taken together, the velocity datasets show consistent ranking of configurations: reinforced triangular UCD provides the largest reduction, followed by the triangular UCD, with the unprotected pier producing the highest velocities. This ranking anticipates corresponding differences in scour depth and scour-hole geometry. The next section examines whether these hydrodynamic modifications translate into measurable reductions in local scour depth and changes in scour/deposition patterns around the pier.

B. Local Scour Response and Mitigation Performance

Scour depth profiles were obtained after each experimental run by comparing post-test bed elevations with the initial level bed along the pier centerline (P1–P12). Qualitative visualizations of the scour hole geometry were produced for both baseline and protected configurations. Under baseline conditions at discharge Q1, the maximum scour depth reached 6.1 cm (Tables IV and V), forming a pronounced scour hole in the upstream and near-pier regions. Following the installation of porous-tube UCDs, the maximum scour depth decreased to 3.3 cm for the reinforced triangular configuration and 3.5 cm for the triangular configuration (Tables VI and VII), corresponding to reductions of 45.9% and 42.6% relative to the

unprotected pier. Representative scour patterns for the protected configurations are presented in Figures 10–12, whereas the longitudinal scour depth comparison along the pier centerline is summarized in Figure 13.

TABLE IV. LONGITUDINAL SCOUR DEPTH (DS) AROUND THE PIER FOR DISCHARGE Q1

Measuring distance	Bridge pillar	Reinforced triangular RCD	Triangular RCD
	Scour depth (cm)		
P1	-6.0	-3.2	-3.5
P2	-6.1	-3.3	-3.3
P3	-5.8	-3.1	-3.1
P4	-5.7	-3.0	-3.0
P5	-4.5	-3.0	-2.4
P6	-3.0	-1.3	-0.6
P7	-0.9	0.3	0.4
P8	-0.5	-0.2	0.1
P9	-2.6	-1.2	-0.4
P10	-3.9	-1.8	-1.4
P11	-4.6	-2.4	-2.1
P12	-5.6	-2.8	-3.2

TABLE V. SCOUR DEPTH MEASUREMENTS BEFORE UCD MODEL PLACEMENT

No	Scour depth (cm)	Scour length (cm)
P1	-6.0	10.0
P2	-6.1	9.2
P3	-5.8	8.9
P4	-5.7	8.9
P5	-4.5	6.1
P6	-3.0	6.0
P7	-0.9	6.0
P8	-0.5	5.3
P9	-2.6	5.8
P10	-3.9	8.2
P11	-4.6	10.0
P12	-5.6	10.4

TABLE VI. SCOUR DEPTH MEASUREMENTS FOR TRIANGULAR UCD AT DISCHARGE Q1

No	Scour depth (cm)	Scour length (cm)
P1	-3.5	6.5
P2	-3.3	5.8
P3	-3.1	5.7
P4	-3.0	5.5
P5	-2.4	3.7
P6	-0.6	3.4
P7	0.4	0
P8	0.1	0
P9	-0.4	4.2
P10	-1.4	6.1
P11	-2.1	6.4
P12	-3.2	7.1

The reduction in scour depth after the placement of the triangular UCD model indicates its effectiveness in mitigating erosive forces around the bridge pier. By reducing the flow velocity, the deflector model weakens the vortices and lessens scouring, which is crucial for protecting structural integrity. This outcome also suggests that the triangular UCD Reinforced model is more efficient at controlling sediment movement, improving the stability of bridge foundations, and preventing structural damage from erosion.

TABLE VII. SCOUR DEPTH MEASUREMENTS FOR REINFORCED TRIANGULAR UCD AT DISCHARGE Q1

No	Scour depth (cm)	Scour length (cm)
P1	-3.2	6.9
P2	-3.3	6.4
P3	-3.1	6.2
P4	-3.0	5.9
P5	-3.0	4.1
P6	-1.3	3.5
P7	0.3	0.0
P8	-0.2	2.8
P9	-1.2	3.3
P10	-1.8	3.0
P11	-2.4	4.9
P12	-2.8	5.1

The Q1 scour profiles indicate that the UCDs not only reduce maximum depth but also limit downstream propagation of the scour hole. Several downstream stations exhibit reduced scour or slight deposition under protected conditions, suggesting redistribution of bed shear and sediment transport capacity downstream of the deflector. The reinforced triangular UCD produces the shallowest minimum and a flatter downstream recovery, consistent with stronger attenuation of near-bed flow and reduced vortex-driven sediment extraction at the pier base. This demonstrates that the triangular UCD models effectively reduce scour depth around the bridge pier. Both the triangular UCD and reinforced triangular UCD models result in a significant decrease in scour, with the reinforced model showing slightly less scour. These findings suggest that the proposed UCDs are effective in mitigating the erosive forces acting on the pier, with the reinforced model providing better protection by further reducing the scour depth. This reduction in scour depth is essential for enhancing the stability and longevity of the bridge structure.

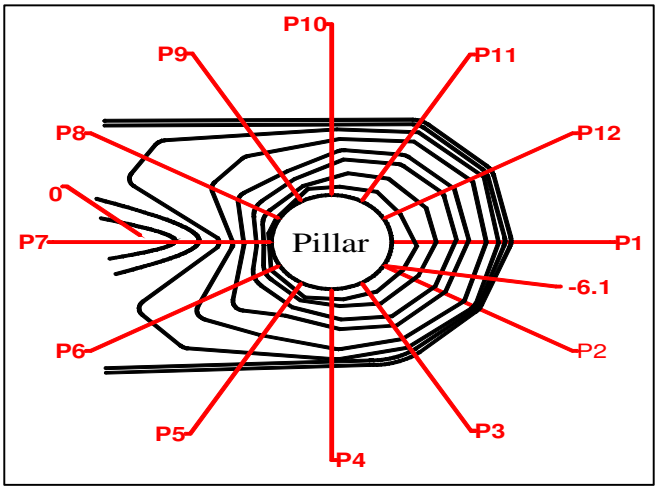

Fig. 10. Local scour around the unprotected pier for discharge Q1.

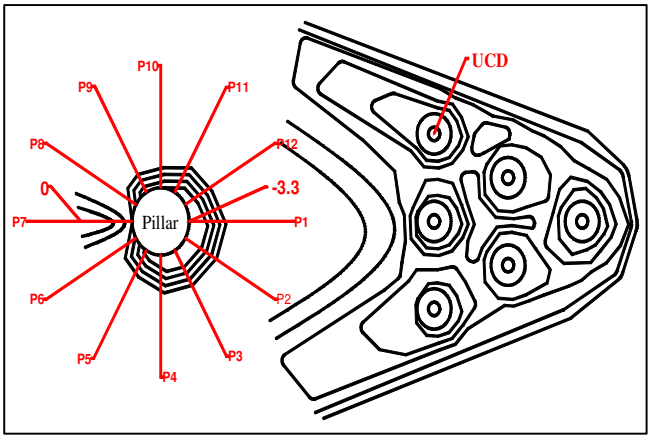

Fig. 11. Local scour around the pier with the reinforced triangular UCD for discharge Q1.

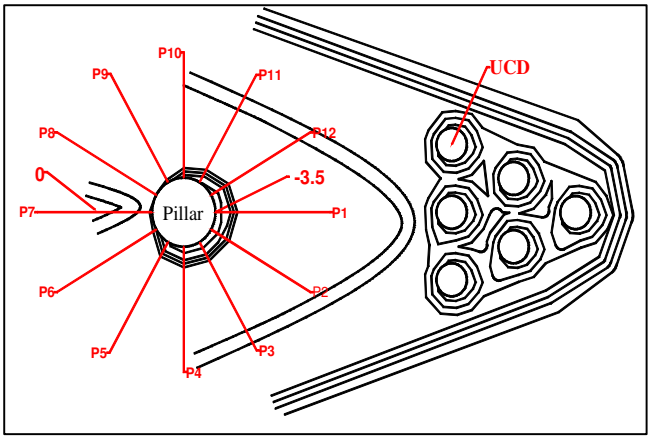

Fig. 12. Local scour around the pier with triangular UCD for discharge Q1.

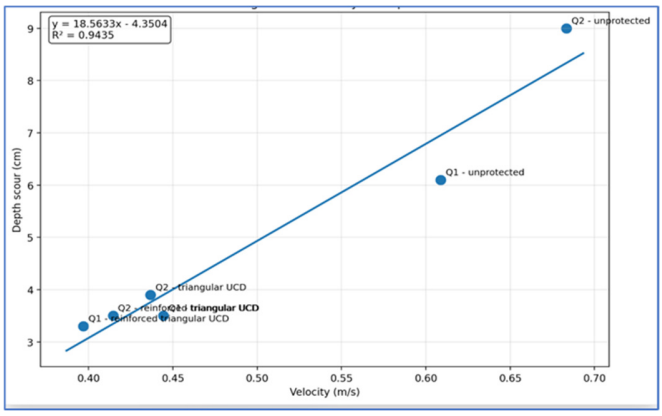

Fig. 13. Relationship between centerline-averaged longitudinal velocity and maximum scour depth for all experimental conditions.

According to Figure 13, which shows the scour depth in the longitudinal direction, before and after the placement of the UCD models, the scour depth at the bridge pier was -6.1 cm. After the placement of the reinforced triangular UCD model, the scour depth reduced to -3.2 cm, whereas the triangular UCD model resulted in a scour depth of -3.5 cm.

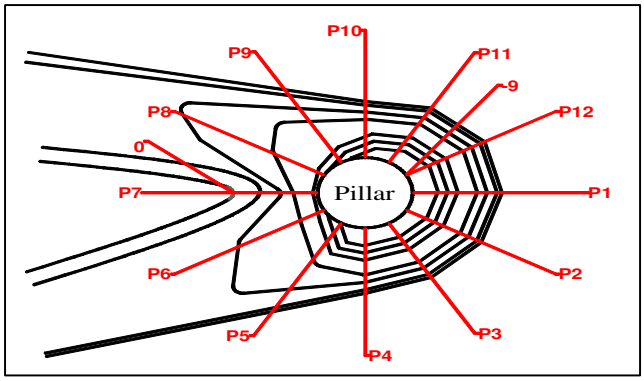

Fig. 14. Local scour around the unprotected pier for discharge Q2.

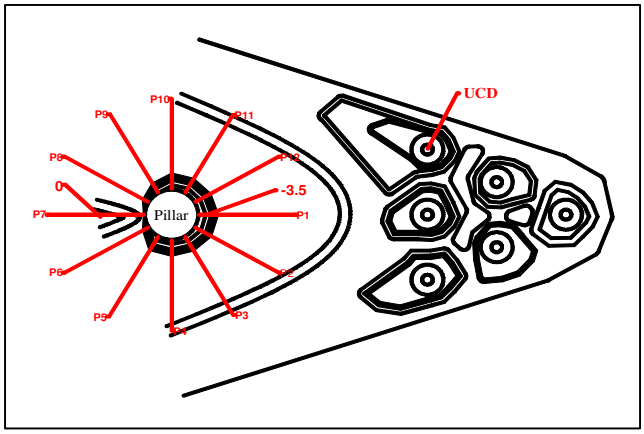

Fig. 15. Local scour around the pier with the reinforced triangular UCD for discharge Q2.

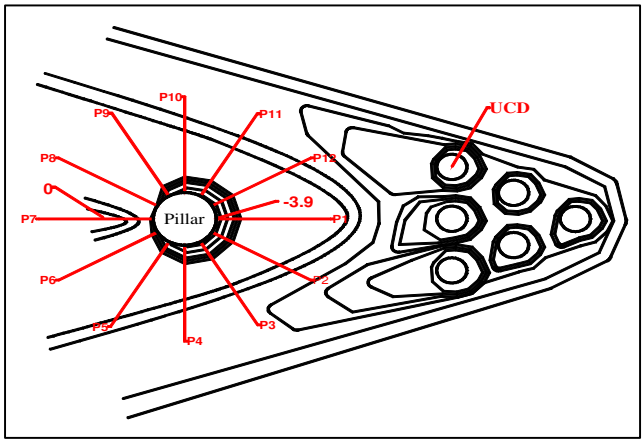

Fig. 16. Local scour around the pier with triangular UCD for discharge Q2.

From the comparison of the scour depth graphs, it can be concluded that the reinforced triangular UCD model is more effective than the triangular UCD model. The reduction in scour depth demonstrates the reinforced model's enhanced performance in mitigating erosive forces around the bridge pier, providing better protection and contributing to the long-term stability of the structure. At the higher discharge Q2, the baseline scour intensified, with a maximum depth of 9.0 cm (Table VIII) and a visibly larger scour hole. With UCD

protection, the maximum scour depth decreased to 3.5 cm (reinforced) and 3.9 cm (triangular), as shown in Tables IX and X, corresponding to reductions of 61.1% and 56.7% relative to the unprotected pier. The scour pattern for the unprotected pillar is illustrated in Figure 14, whereas Figures 15 and 16 demonstrate the scour pattern for the protected pillars. The comparative longitudinal profiles are portrayed in Figure 17.

TABLE VIII. LONGITUDINAL SCOUR DEPTH (DS) AROUND THE PIER FOR DISCHARGE Q2

Measuring distance	Bridge pillar	Reinforced triangular RCD	Triangular RCD
	Scour depth (cm)		
P1	-8.9	-3.5	-3.9
P2	-8.6	-3.4	-3.8
P3	-8.4	-3.1	-3.8
P4	-8.8	-3	-3.5
P5	-8.8	-3	-2.3
P6	-5.0	-1	-1.0
P7	-4.6	0	0.4
P8	-5.0	-1	-0.1
P9	-6.1	-2	-2.0
P10	-7.5	-3	-2.9
P11	-8.4	-3.1	-3.3
P12	-9.0	-3.2	-3.8

TABLE IX. SCOUR DEPTH MEASUREMENTS FOR TRIANGULAR UCD AT DISCHARGE Q2

No	Scour depth (cm)	Scour length (cm)
P1	-3.9	7.7
P2	-3.8	7.3
P3	-3.8	6.4
P4	-3.5	6.4
P5	-2.3	4.5
P6	-1.0	4.3
P7	0.4	0.0
P8	-0.1	4.0
P9	-2.0	4.8
P10	-2.9	6.9
P11	-3.3	7.2
P12	-3.8	7.6

TABLE X. SCOUR DEPTH MEASUREMENTS FOR REINFORCED TRIANGULAR UCD AT DISCHARGE Q2

No	Scour depth (cm)	Scour length (cm)
P1	-3.5	7.4
P2	-3.4	6.9
P3	-3.1	6.6
P4	-3.0	7.0
P5	-3.0	4.5
P6	-1.0	4.1
P7	0	0
P8	-1.0	4.2
P9	-2.0	4.8
P10	-3.0	7.7
P11	-3.1	7.1
P12	-3.2	7.4

The results indicate that prior to the installation of the UCD, the scour depth around the bridge pier was significantly high. The measurements highlight the pier's vulnerability to erosion under the given flow conditions, underscoring the need for interventions such as the UCD to mitigate scour and protect the structure.

The effectiveness of the reinforced triangular UCD model is evident, as it prevents further sediment erosion, which is significant for preserving the integrity of the bridge foundation. This outcome shows that the reinforced triangular UCD model is more successful in mitigating scour compared to other models, ultimately enhancing the protection of bridge structures from the damaging effects of strong flow currents.

Figure 17 shows the longitudinal scour depth before and after the placement of the UCD models. The scour depth at the unprotected pier was -9 cm. After installing the reinforced triangular UCD model, the highest scour depth was -3.5 cm, whereas the triangular UCD model yielded a scour depth of -3.9 cm.

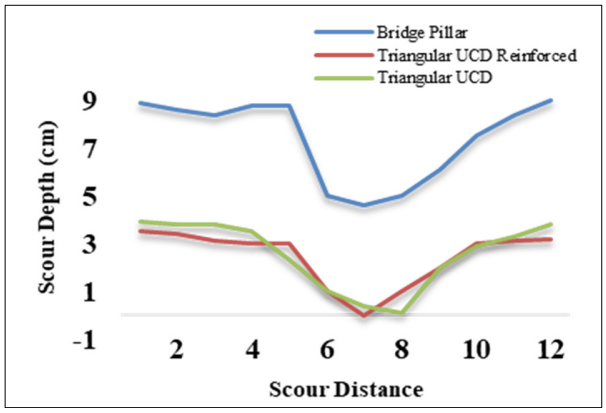

Fig. 17. Comparison of longitudinal scour depth profiles for discharge Q2.

Based on the comparison of the scour depth graphs, the reinforced triangular UCD model is more effective than the triangular UCD model. Across both discharges, porous-tube UCD consistently reduced longitudinal velocity and maximum scour depth, with the reinforced triangular configuration producing the greatest reduction. The relative reduction in maximum scour depth increased at the higher discharge Q2, suggesting that velocity-driven intensification of baseline scour is more effectively counteracted when the deflector maintains structural stability and sustained momentum dissipation under stronger flow. These trends provide a velocity-dependent basis for selecting porous-tube UCD configurations for practical scour-mitigation applications.

IV. DISCUSSION

Porous-tube UCDs reduced near-bed longitudinal velocity and maximum local scour depth around the cylindrical pier under both discharge conditions. This behavior is consistent with the established scour mechanism, in which near-bed acceleration, downflow, and the horseshoe vortex system control sediment entrainment at the pier base. The observed scour reduction with porous-tube UCD installations can be attributed to three interacting mechanisms: momentum dissipation, vortex modification, and shear stress redistribution.

In the unprotected configuration, increasing the discharge from Q1 to Q2 increased the maximum scour depth from 6.1 cm to 9.0 cm, confirming that hydraulic intensity is the primary driver of scour development. The observed scour reduction

with UCD installation is attributed to momentum dissipation within the porous array, redirection of near-pier streamlines that reduces shear-stress concentration at the pier toe, and partial flow transmission that limits stagnation-induced contraction jets while promoting downstream bed stability.

Across both discharge conditions, the reinforced triangular UCD configuration produced the smallest maximum scour depth and the largest velocity reduction. Its advantage was more pronounced at Q2, where maximum scour decreased by approximately 61%, compared with about 57% for the unreinforced triangular configuration. The improved performance likely results from enhanced structural stability that preserves the intended porosity distribution and flow-deflection geometry under higher hydrodynamic loading. These results indicate that scour mitigation arises primarily from localized modifications to near-pier velocity gradients and vortex structures rather than from a uniform reduction in approach velocity.

The strong discharge sensitivity of baseline scour highlights persistent uncertainty in pier-scour prediction and underscores the importance of controlled laboratory experiments for benchmarking protective measures. Although the pier geometry remained fixed, the UCD installation effectively altered the hydraulic footprint of the structure by modifying the local flow field around the pier. This finding aligns with previous studies showing that geometric flow-modifying devices significantly influence vortex development and the associated scour patterns.

Porous-tube UCDs, therefore, complement existing structural countermeasures by modifying the approach flow and partially shielding the pier toe, offering a permeable and modular retrofit option for bridge foundations. The selection of mitigation strategies should consider scour reduction requirements, constructability, maintenance needs, and environmental constraints.

Several limitations should be noted. The experiments considered only two discharge conditions with fixed pier and sediment properties, and velocity measurements were limited to selected stations. Field complexities, such as debris accumulation, skewed approach flows, wave effects, and live-bed sediment supply, were not represented. Therefore, future studies should extend the hydraulic range, incorporate live-bed conditions and sediment feeding, and evaluate debris interaction, clogging potential, oblique flows, and alternative pier geometries. Coupling physical experiments with validated numerical simulations would further support parametric analysis and the development of practical design guidelines.

V. CONCLUSIONS

This study evaluated porous-tube Underwater Current Deflectors (UCDs) as a practical countermeasure for bridge-pier scour under two discharges (Q1 and Q2) representing increasing flow velocity. Two configurations, triangular and reinforced triangular UCDs, were assessed using laboratory flume experiments that measured the longitudinal velocity (P1–P15) and post-test scour depth distributions (P1–P12). Both porous-tube UCDs reduced longitudinal velocities downstream of the pier and reduced maximum scour depth relative to the unprotected pier. The spatially averaged longitudinal velocity reduction ranged from approximately 27–35% at Q1 and 36–39% at Q2. The maximum scour depth decreased from 6.1 cm (Q1) and 9.0 cm (Q2) for the unprotected pier to 3.3–3.5 cm at Q1 and 3.5–3.9 cm at Q2 for the protected cases. The reinforced triangular UCD consistently produced the lowest maximum scour depth and the highest overall velocity attenuation, indicating improved robustness and sustained performance at higher velocities.

From a practical perspective, porous tube UCDs offer an installable, potentially retrofittable solution that mitigates scour through localized flow modification rather than full-bed armoring. Reinforcement should be prioritized in high-velocity environments to maintain device geometry and effective porosity under higher hydrodynamic loading. Future studies should evaluate performance under live-bed transport, variable sediment supply, debris accumulation/clogging, and oblique approach flow, and should couple laboratory results with validated numerical modeling to develop transferable design guidance for field-scale implementation. These findings suggest that porous-tube UCDs can serve as a practical and hydraulically efficient scour-mitigation strategy for bridge piers exposed to high-velocity flows.

DECLARATION OF COMPETING INTERESTS

The authors declare no competing interests.

ACKNOWLEDGMENT

The authors acknowledge the support of the Department of Water Resources Engineering, Universitas Muhammadiyah Makassar, for providing laboratory facilities and technical assistance during the flume experiments. This research received no funding.

DATA AVAILABILITY

The dataset used in this research can be accessed at [18].

AI USE AND DECLARATION OF GENERATIVE AI USE

During the preparation of this article, the authors used Quillbot and GPT to enhance the article's sentence quality.

REFERENCES

[1] M. Esmaeili Varaki, N. Tavazo, and A. Radice, "Using a Bed Sill as a Countermeasure for Clear-Water Scour at a Complex Pier with Inclined Columns Footed on Capped Piles," *Hydrology*, vol. 9, no. 4, Apr. 2022, Art. no. 65, https://doi.org/10.3390/hydrology9040065.

[2] G. Crotti and S. Manzoni, "In-field assessment of bridge pier scour by means of Fiber Bragg Gratings: System and algorithms," *Measurement*, vol. 242, Jan. 2025, Art. no. 116030, https://doi.org/10.1016/j.measurement.2024.116030.

[3] Harshvardhan and D. R. Kaushal, "Equilibrium scour pattern around tandem piers at an intermediate below-critical inflow velocity," *Journal of Hydrology and Hydromechanics*, vol. 73, no. 4, pp. 412–442, Dec. 2025, https://doi.org/10.2478/johh-2025-0032.

[4] M. Baduna Koçyiğit and Ö. Koçyiğit, "Experimental Investigation of Bridge Scour under Pressure Flow Conditions," *Water*, vol. 16, no. 19, Sept. 2024, Art. no. 2773, https://doi.org/10.3390/w16192773.

[5] F. Gumgum and M. S. Guney, "Effect of Sediment Feeding on Live-Bed Scour around Circular Bridge Piers," *Civil Engineering Journal*, vol. 7, no. 5, pp. 906–914, May 2021, https://doi.org/10.28991/cej-2021-03091699.

[6] M. Annad and A. Lefkir, "Analytic network process for local scour formula ranking with parametric sensitivity analysis and soil class clustering," *Water Supply*, vol. 22, no. 11, pp. 8287–8304, Nov. 2022, https://doi.org/10.2166/ws.2022.357.

[7] A. Choudhary, B. S. Das, K. Devi, and J. R. Khuntia, "ANFIS- and GEP-based model for prediction of scour depth around bridge pier in clear-water scouring and live-bed scouring conditions," *Journal of Hydroinformatics*, vol. 25, no. 3, pp. 1004–1028, May 2023, https://doi.org/10.2166/hydro.2023.212.

[8] S. M. Abdelalim, M. A. Gad, and D. A. El-Molla, "Modeling local scour around complex bridge supports using CFD and a shear-stresses-based simplified approach," *Journal of Engineering and Applied Science*, vol. 71, Dec. 2024, Art. no. 208, https://doi.org/10.1186/s44147-024-00544-1.

[9] R. Maimun, Abdullah, Nizarli, and Safwan, "Experimental study on Local Scour around Bridge Pier Models generated by Flash Floods carrying Debris," *IOP Conference Series: Earth and Environmental Science*, vol. 1343, May 2024, Art. no. 012028, https://doi.org/10.1088/1755-1315/1343/1/012028.

[10] E. Affandy, M. S. Pallu, F. Maricar, and B. Bakri, "An Experimental Study on Local Scour Protection for Round Slotted Bridge Piers with Collar Variations," *Engineering, Technology & Applied Science Research*, vol. 15, no. 6, pp. 29685–29695, Dec. 2025, https://doi.org/10.48084/etasr.14582.

[11] F. Bangnira, B. Marti-Cardona, B. Imam, and V. Ruiz-Villanueva, "Identifying bridges prone to instream wood accumulation: insights from bridges across the UK," *Natural Hazards*, vol. 120, no. 1, pp. 25–40, Jan. 2024, https://doi.org/10.1007/s11069-023-06174-9.

[12] M. S. Al-Khafaji, L. Abdulameer, A. T. Al-Awadi, N. M. L. Al Maimuri, and A. N. Al-Dujaili, "Investigating the scour at piers of successive bridges with debris accumulation," *Journal of Infrastructure Preservation and Resilience*, vol. 6, July 2025, Art. no. 23, https://doi.org/10.1186/s43065-025-00138-y.

[13] C. S. Silvia, M. Ikhsan, and A. Azwanda, "Effect Of Bridge Piers On Local Scouring At Alue Buloh Bridge Nagan Raya Regency," *Journal of the Civil Engineering Forum*, vol. 7, no. 1, pp. 37–46, Sept. 2020, https://doi.org/10.22146/jcef.57719.

[14] N. Nenny, F. Daud S., S. Antaria, and H. A. Imran, "The Effect of Flow Velocity on Bridge Pillar Concrete Wings Using iRIC Software Nays2HD 3.0.," *Civil Engineering and Architecture*, vol. 10, no. 2, pp. 620–631, Mar. 2022, https://doi.org/10.13189/cea.2022.100218.

[15] I. H. S. Al-Rahoo and N. K. Alomari, "Using a Curved Bed Sill as a Scour Countermeasure around a Complex Bridge Pier," *Tikrit Journal of Engineering Sciences*, vol. 32, no. 1, Mar. 2025, Art. no. 1553, https://doi.org/10.25130/tjes.32.1.7.

[16] S. A. M. Darzikolaei and X. Liu, "Scour Around Porous and Solid Structures: Sediment Transport, Porosity Effects, and Semi-Theoretical Scour Evolution Model," *Water Resources Research*, vol. 61, no. 11, Nov. 2025, Art. no. e2025WR040894, https://doi.org/10.1029/2025WR040894.

[17] R. Farshad, S. M. Kashefipour, M. Ghomeshi, and G. Oliveto, "Temporal Scour Variations at Permeable and Angled Spur Dikes under Steady and Unsteady Flows," *Water*, vol. 14, no. 20, Oct. 2022, Art. no. 3310, https://doi.org/10.3390/w14203310.

[18] Nenny, "Dataset of research The effect of flow velocity on the effectiveness of porous tubes," Apr. 2026. doi.org/10.6084/m9.figshare.32101360.